Sensitivity and Uncertainty Analysis of a Zoonotic Continuous-Time Markov Chain SEIR-κ Model for Marburg Virus Disease

Erin Xu

2026-04-03

Introduction

In the RNA virus family *Filoviridae*, Marburg virus (MARV) and Ravn virus (RAVV) are causative agents of Marburg virus disease (MVD), which is recognized as an important priority in WHO emergency research and outbreak preparedness contexts (World Health Organization, 2026b). MVD outbreaks produce severe viral hemorrhagic fever, often ending with multiorgan failure and shock, with high case-fatality rates (CRFs).

While rare and understudied, they remain a major public health burden in sub-Saharan Africa because of high pathogenicity with potential for geographic spread through regional mobility and international travel, general lack of medical countermeasures and recurrent zoonotic spillover. For example, the largest MARV outbreak reported to date occurred in 2004 in Angola, with 374 reported cases and 329 deaths – a CFR of 88% (World Health Organization, 2026a).

The handling of filoviruses is restricted to biosafety level 4 (BSL4) facilities, which require significant resources to maintain and complicate the development of any assay reagents. There are no specific post-exposure treatments, such as post-exposure prophylaxis (PEP), and post-MVD complications are generally unstudied, although preclinical trials of several vaccines through nonprofit organizations are currently in rapid development (IAVI, 2026).

Outbreaks are typically initiated by zoonotic spillover, in which infections are introduced from wildlife into humans. MARV has a confirmed reservoir in the Egyptian rousette bat *Rousettus aegyptiacus*, which shed the virus in saliva and urine. Humans may encounter bats in mining and cave tourism activities and inhale or directly contact such contaminated excreta. Following spillover, transmission is driven primarily by close contact with infectious bodily fluids, making household caregiving and healthcare settings high-risk contexts, and there have also been noticeable transmission instances from exposure in healthcare and laboratory settings (Soni & Rathish, 2026).

MVD presents a particular challenge for inference because outbreaks are rare and the available data are sparse, with limited case counts, incomplete transmission records, and uncertainty in spillover frequency. In this setting, stochastic variability is especially important, making sensitivity and uncertainty analysis central to model interpretation.

Therefore, the goal of this study is to examine how plausible variation in epidemiological parameters affect the probability, size, duration, and severity of Marburg virus outbreaks in a stochastic zoonotic SEIR-κ model; in particular, under what conditions an outbreak dies out rather than develops into a large epidemic, and which regions of parameter space are associated with large or sustained outbreaks. Plausible ranges are chosen for the exposed-to-infectious rate σ, the removal rate γ, the basic reproduction number R_0, the corresponding transmission rate $\beta = R_0\gamma$ and, in the repeated-spillover setting, the spillover intensity κ. These parameter ranges are sampled using a hybrid Latin Hypercube Sampling (LHS) approach, and stochastic outbreak trajectories are simulated using the Gillespie algorithm. Outbreak statistics relevant to epidemiology are computed, including outbreak probability, extinction probability, final outbreak size, outbreak duration, and peak number infectious. Sensitivity analysis, through partial rank correlation coefficients (PRCC), is then used to determine which parameters most strongly influence these outcomes.

Literature Review

Mathematical modelling of MVD remains relatively limited compared with modelling work for other high-consequence pathogens, but the existing literature provides several useful foundations for the present study.

A recent systematic review by Cuomo-Dannenburg et al. (2024) extracted 221 peer-reviewed papers reporting historical outbreaks, modelling studies and epidemiological parameters, and published their database of extracted MVD models, parameters and outbreaks. The epidemiological parameter estimates cover seroprevalence estimates, transmission parameters (attack rates and reproduction numbers), reported risk factors for different outcomes (infection, severe disease, seropositivity, recovery, and death). Only 1 reproduction number and 6 CFR estimates were found, and only for specific outbreak events. Papers on transmission parameters had on average the highest quality assessment scores, and papers on seroprevalence had some of the lowest scores. In summary, Marburg modelling literature is still sparse and key epidemiological parameters for MVD remain poorly estimated.

There was only 1 transmission modelling study of MVD, done by Ajelli & Merler (2012). The authors estimated $R_0 = 1.59$ with a 95% confidence interval of $(1.53, 1.66)$ for the largest known outbreak to date in Angola with an individual-based discrete-time stochastic Markov chain SEIR-like model. First, estimation of the probability density function (PDF) $\omega(t)$ of the generation time T_g (how likely transmission to a secondary case is to occur t days after the primary infection) occurs. Assuming infectiousness over time is proportional to viral load, a gamma distribution with an offset to viral load data is fit. After adjusting for the high CFR, $\omega(t)$ has mean of 9 days and standard deviation 5.4 days. Then, the authors assume that the early phase of the outbreak grows exponentially, to estimate the growth rate of the cumulative number of MARV infections observed during the early phases, r. This can be calculated with $C(t) \approx C_0 e^{rt}$, where $C(t)$ is the number of cases at time t, C_0 is the initial number of cases, and r is the exponential growth rate. They estimated $r = 0.056$ days^{-1} with 95% confidence interval $(0.0508, 0.0612)$. Finally, $R_0 = \frac{1}{\int_0^\infty e^{-rt} w(t)\, dt}$, is the Laplace transform of the generation time distribution evaluated at r, a weighted average of e^{-rt} across all possible generation times. Their analysis suggested that MARV outbreaks are characterized by a relatively small reproduction number, a comparatively long estimated average generation time, infections result in a fatal outcome with a median of 7 days, and that timely case isolation can substantially reduce outbreak size.

More recently, Qian et al. (2023) developed a general branching-process model of MVD transmission to study the potential role of vaccination strategies under different outbreak conditions (zoonotic spillover introductions or human-to-human onward transmission). They simulate outbreaks under different vaccination strategies and intervention timings. They informed the model using line-list data from the 15 recorded outbreaks up to 2022 and an Approximate Bayesian Computation (ABC) framework for parameter estimation. Their estimated rate of zoonotic introductions was 0.06 and 0.003 per day during the DRC and Angola outbreaks, respectively. Across all outbreaks, the median delay between onset of the first MVD case and beginning of interventions was 21 days, and a gamma distribution was found to best fit the MVD serial intervals that is comparable to Ajelli & Merler (2012). They also concluded that for the majority of outbreaks, the median value of R_0 was less than 1, lower than estimates from Ajelli & Merler (2012).

Beyond Marburg-specific studies, a broader mathematical epidemiology literature motivates the use of stochastic compartmental models for rare zoonotic outbreaks. Allen (2017) provides a general framework for formulating epidemic models as CTMCs and for simulating them numerically using event-driven methods such as the Gillespie algorithm. These ideas are directly aligned with MVD, where outbreaks often begin with a small number of spillover-linked cases and early transmission chains may either fade out or generate wider spread. Related work on zoonotic disease modelling has also stressed the importance of explicitly representing wildlife-to-human transmission. Allen et al. (2012) and Odatalla (2020) cover population-level models (reaction–diffusion models, and patch/metapopulation models) for contact and transmission. The baseline method is the standard SIR/SIS-type compartmental framework to study quantities such as the probability of an outbreak, final size distribution, epizootic duration, and fade-out/persistence. This is especially relevant for wildlife zoonoses because data are sparse and failed outbreaks may go unobserved.

Taken together, the existing literature suggests three motivations for the present study: Marburg-specific parameter estimates remain limited, stochastic formulations are more suitable than deterministic models for extinction and outbreak variability, and repeated zoonotic spillover may materially shape outbreak dynamics. This motivates a stochastic SEIR-κ framework with uncertainty analysis across plausible parameter ranges.

Model Formulation

To simplify the system enough to permit simulation and sensitivity analysis, while retaining the central biological features of MVD relevant to outbreak dynamics, the model relies on the following assumptions: the total human population is assumed constant over the outbreak timescale; human-to-human transmission follows homogeneous mass-action mixing with transmission rate β; exposed individuals are infected but not yet infectious, with infection arising either through human-to-human transmission or through zoonotic introduction from the reservoir; σ is the rate of progression from exposed to infectious; infectious individuals leave the infectious compartment at rate γ, by recovery or death; zoonotic spillover occurs according to an external rate κ; waiting times for progression and removal are exponentially distributed, so the process is Markovian; and there are no interventions, behavioural changes, or spatial structure explicitly included.

At time t, each human individual belongs to one of four epidemiological classes:

$$S(t) = \text{susceptible} \qquad E(t) = \text{exposed} \qquad I(t) = \text{infectious} \qquad R(t) = \text{removed}$$

The deterministic mean-field analogue:

$$\frac{dS}{dt} = -\beta\frac{SI}{N} - \kappa S \tag{1}$$

$$\frac{dE}{dt} = \beta\frac{SI}{N} + \kappa S - \sigma E \tag{2}$$

$$\frac{dI}{dt} = \sigma E - \gamma I \tag{3}$$

$$\frac{dR}{dt} = \gamma I \tag{4}$$

$$N = S(t) + E(t) + I(t) + R(t) \tag{5}$$

Parameter	Meaning	Units	Interpretation / source
β	human-to-human transmission rate	day^{-1}	often derived from R_0 and γ
σ	progression rate from exposed to infectious	day^{-1}	inverse of latent/incubation timescale
γ	removal rate from infectious to removed	day^{-1}	inverse of infectious/removal timescale
κ	zoonotic spillover rate	day^{-1}	scenario-based external introduction rate
N	total human population	persons	assumed constant

Table 1: Model parameters.

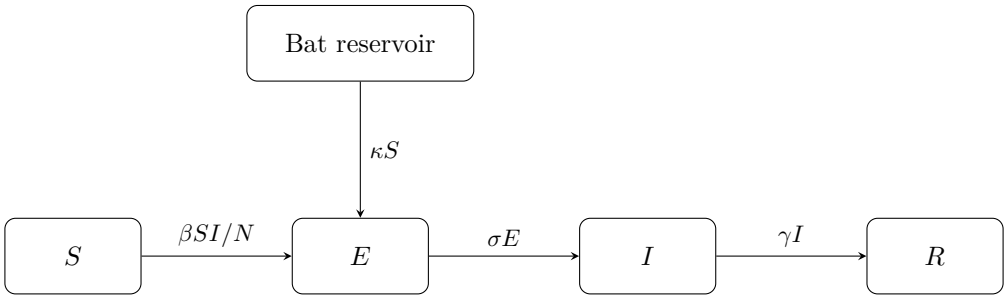

Figure 1: Compartment structure of the CTMC SEIR-κ model.

To account for demographic stochasticity, the model is formulated as a CTMC. Let

$$X(t) = (S(t), E(t), I(t), R(t))$$

denote the state of the process at time t. The state space is

$$\mathcal{S} = \{(s, e, i, r) \in \mathbb{Z}^4_{\geq 0} : s + e + i + r = N\}$$

The process evolves through three distinct state changes arising from four biologically meaningful events: human-to-human infection, zoonotic spillover, progression from exposed to infectious, and removal. For a sufficiently small time interval $\Delta t > 0$, the infinitesimal transition probabilities are:

$$\begin{aligned}
&\mathbb{P}((S,E,I,R)(t+\Delta t) = (s-1, e+1, i, r) \mid (S,E,I,R)(t) = (s,e,i,r)) \\
&\quad = \left(\beta \frac{si}{N} + \kappa s\right) \Delta t + o(\Delta t) \\
&\mathbb{P}((S,E,I,R)(t+\Delta t) = (s, e-1, i+1, r) \mid (S,E,I,R)(t) = (s,e,i,r)) = \sigma e\, \Delta t + o(\Delta t) \\
&\mathbb{P}((S,E,I,R)(t+\Delta t) = (s, e, i-1, r+1) \mid (S,E,I,R)(t) = (s,e,i,r)) = \gamma i\, \Delta t + o(\Delta t) \\
&\mathbb{P}((S,E,I,R)(t+\Delta t) = (s, e, i, r) \mid (S,E,I,R)(t) = (s,e,i,r)) \\
&\quad = 1 - \left(\beta \frac{si}{N} + \kappa s + \sigma e + \gamma i\right) \Delta t + o(\Delta t)
\end{aligned}$$

where $o(\Delta t)$ denotes higher-order terms such that $o(\Delta t)/\Delta t \to 0$ as $\Delta t \to 0$.

Model Justification

A stochastic CTMC SEIR-κ model is used to capture two key features of MVD outbreak dynamics: a latent period between infection and infectiousness (E), and zoonotic spillover (κ) from the animal reservoir into the human population. This allows the model to represent both single introductions and repeated spillover events.

The use of a CTMC formulation accounts for demographic stochasticity, extinction probabilities and variability in outbreak trajectories that cannot be captured by deterministic models alone (Allen, 2017).

For analytical tractability, a single-introduction scenario with $\kappa = 0$ after the initial spillover is considered when deriving early-phase outbreak probabilities. This isolates human-to-human transmission dynamics and allows the use of a branching process approximation near the disease-free equilibrium. Qian et al. (2023) shows that there are various outbreak conditions across known cases.

Finally, standard incidence $\beta SI/N$ is used to reflect frequency-dependent transmission, appropriate for human populations where contact rates do not scale linearly with population size. Together, these modeling choices provide a balance between biological realism and mathematical tractability.

The model is intended as an exploratory stochastic transmission model for human outbreaks seeded by spillover, rather than an predictive or full ecological and clinical description of MVD. Its main purpose is to understand how repeated zoonotic introduction changes outbreak variability, persistence, and sensitivity structure relative to a single-introduction scenario.

Methodology

Sample paths of the stochastic model are generated using the Gillespie stochastic simulation algorithm. This algorithm is a natural choice because it exactly simulates trajectories of a CTMC by drawing the waiting time to the next event from an exponential distribution determined by the total event rate, and then selecting which event occurs according to the relative transition rates. In the present model, this allows direct simulation of outbreak realizations under both human-to-human transmission and spillover-driven infection.

To study early outbreak behavior, a branching process approximation is applied near the disease-free equilibrium (DFE) in the single-introduction setting, where an initial spillover event seeds the outbreak and subsequent transmission is assumed to occur only between humans. This restriction is necessary because if $\kappa > 0$ is maintained continuously, the disease-free state is no longer absorbing and classical extinction and major-outbreak results do not apply directly. Within the single-introduction setting, the basic reproduction number $R_0 = \frac{\beta}{\gamma}$

is used as a summary statistic governing whether sustained transmission is possible. The same threshold is confirmed using the next-generation matrix (NGM) for the infected compartments (E, I), so that the branching process approximation and deterministic threshold analysis are consistent.

After the model structure was established, biologically plausible parameter values and uncertainty ranges were explored using a hybrid LHS sampling design, with ranges specified using published literature and scenario-based assumptions (Table 2). This is because direct Marburg-specific estimates are extremely limited, as there have been fewer than 20 reported outbreaks in history; the literature review found 2 values for R_0 with confidence intervals (World Health Organization, 2026a). More broadly, this reflects a no free lunch problem in rare-outbreak parameterization: with such limited data, no single estimation approach can be expected to dominate. If competing methods are all biologically plausible and grounded in the same sparse evidence base, they should generally perform similarly, with differences arising mainly from how each method encodes assumptions and handles uncertainty. Accordingly, broad continuous ranges are adopted, and LHS is used to propagate that uncertainty through the model rather than overcommitting to a sparse set of point estimates.

The continuously sampled inputs were assigned broad continuous uniform distributions over literature- and scenario-informed bounds (census): $T_E \sim \text{Unif}(2, 21)$, $T_I \sim \text{Unif}(5, 16)$, $R_0 \sim \text{Unif}(0.50, 1.59)$, and $N \sim \text{Unif}(25{,}000, 1.14 \times 10^6)$. The use of uniform distributions reflects an intentionally weak prior structure: given the scarcity of Marburg-specific data, there is insufficient basis for imposing more informative within-range weighting. The rate parameters were then computed as $\sigma = 1/T_E$, $\gamma = 1/T_I$, and $\beta = R_0\gamma$.

LHS design was then augmented with a binary mode variable $M \sim \text{Bernoulli}(0.5)$ to address the spillover scenarios, where $M = 0$ corresponds to a single-introduction setting and $M = 1$ corresponds to a continuous-spillover setting. $\kappa = 0$ when $M = 0$, whereas $\kappa \sim \text{Unif}(0.003, 0.079)$ when $M = 1$. This hybrid framework allows the sampling scheme to capture both continuous parameter uncertainty and discrete structural uncertainty in spillover dynamics and alternative outbreak-generating mechanisms.

Quantity	Meaning	Distribution / definition	Units	Role	Source / note
T_E	Latent period	$\text{Unif}(2, 21)$	days	Sampled (LHS)	World Health Organization (2025) for incubation period range
T_I	Infectious / removal period	$\text{Unif}(5, 16)$	days	Sampled (LHS)	European Centre for Disease Prevention and Control (2024) and Carmona (2025) for plausible removal-period range
R_0	Basic reproduction number	$\text{Unif}(0.50, 1.59)$	–	Sampled (LHS)	Borchert et al. (2006), Bausch et al. (2006), Ajelli & Merler (2012), and Qian et al. (2023) define broad outbreak-level estimates
M	Spillover mode	$\text{Bernoulli}(0.5)$	–	Sampled	$M = 0$: single spillover; $M = 1$: continuous spillover; Qian et al. (2023)
κ	Spillover rate	$\kappa = \begin{cases} 0, & M = 0, \\ \text{Unif}(0.003,\ 0.079), & M = 1 \end{cases}$	day^{-1}	Sampled / scenario-dependent	If $M = 0$, one initial spillover event seeds the outbreak and $\kappa = 0$ thereafter; if $M = 1$, κ is sampled over the reported spillover range; Qian et al. (2023) and Bausch et al. (2006)
N	Population at risk	$\text{Unif}(25{,}000,\ 1.14 \times 10^6)$	persons	Sampled (LHS)	Broad range spanning outbreak settings considered; Data Commons (2016) and Bausch et al. (2006)
σ	Progression rate from exposed to infectious	$\sigma = 1/T_E$	day^{-1}	Derived	Computed from sampled latent period
γ	Removal rate from infectious to removed	$\gamma = 1/T_I$	day^{-1}	Derived	Computed from sampled infectious / removal period
β	Human-to-human transmission rate	$\beta = R_0\gamma$	day^{-1}	Derived	Computed from sampled R_0 and γ

Table 2: Model quantities used for uncertainty analysis, for augmented LHS design.

Global sensitivity analysis was carried out using PRCCs. For each sampled parameter set, repeated Gillespie simulations were summarized into outbreak-level response measures, and PRCC was then used to quantify the direction and strength of the monotone association between each input parameter and each output measure while controlling for the remaining parameters. Because PRCC operates on ranks rather than raw values, it is well suited for stochastic epidemic outputs that may be nonlinear or non-normally distributed. PRCCs

were used to identify which parameters had the strongest monotone association with key quantities of interest: mean outbreak size, mean peak prevalence, mean outbreak duration, and the estimated probability of a major outbreak. Because κ is structurally zero under single-introduction scenarios, pooled PRCC analysis would induce design-based collinearity between spillover mode and κ. PRCCs were therefore computed separately for the single-introduction and continuous-spillover subsets, with κ excluded from the former (Figure 2).

This overall structure allows the model to capture both the mechanistic features of Marburg virus transmission and the stochastic variability that is especially important for rare zoonotic outbreaks (see Appendix for code commentary).

Results

Results are reported separately for the single-introduction ($M = 0$) and continuous-spillover ($M = 1$) regimes in order to isolate the effect of repeated zoonotic seeding on outbreak dynamics.

Table 3 confirms that the two regimes were sampled similarly with respect to T_E, T_I, R_0 and N, with the principal structural difference being that for the single-introduction regime, $\kappa = 0$, and $\kappa \geq 0$ for the continuous spillover (Figure 3).

The Gillespie trajectory plots for single spillover (Figure 4) highlights substantial stochastic variability in outbreak behaviour under both regimes. Many realizations remain small and die out relatively quickly, and tend to peak much later (after 2-3 years), and there seems to be a center at around 700 days for peak infection numbers. This is very reasonable because the ranges obtained from Ajelli & Merler (2012), Qian et al. (2023), Bausch et al. (2006), Borchert et al. (2006) follow some this scenario where the outbreak did in fact last over 2 years (such as Angola 2005), with R_0 around 1, so most likely these instances are strong vestiges of those scenarios. At the same time, a smaller subset of realizations produces much larger epidemics with the maximum situation resulting in 40,000 infectious individuals before dying out after 800 days. This indicates that a single spillover event can still generate a substantial outbreak when transmission conditions are favourable, especially as N can be chosen to be very large and the PRCC graph does show a strong correlation between the number of infectious and the population size (Figure 2).

In contrast, the continuous-spillover regime exhibits the classic outbreak behaviour with a peak number of infected individuals at around 75 days and then slowly dying out (Figure 5). This is consistent with the model structure: repeated zoonotic introductions reduce the fragility of early transmission chains and sustain epidemic growth through ongoing external seeding.

This contrast is also reflected in Table 4. Under single introduction, mean outbreak size and peak prevalence far exceed their medians, indicating strongly right-skewed outcomes, whereas under continuous spillover both mean and median values are much larger, showing that repeated spillover shifts the system toward consistently larger outbreaks.

PRCC analysis (Figure 2) showed that mean final size was strongly positively associated with population size N in both regimes. In the continuous-spillover regime, κ had a positive association on final size, while other factors do not noticeably reduce outbreak size as the negative PRCC values are shown to be not significant. Peak prevalence was most strongly associated with R_0, while longer latent periods tended to reduce peak magnitude. Duration behaved differently across regimes: in the single-introduction case, higher R_0 T_E were associated with longer outbreaks, whereas in the continuous-spillover case, higher κ was associated with shorter duration, consistent with faster, more intense epidemic trajectories. Because the major-outbreak probability was nearly always 1 under continuous spillover, that outcome showed little meaningful variation.

Figure 6 and the monotonicity diagnostics (Figures 7–8) show that the single-introduction regime produces more clearly monotone input-output relationships than the continuous-spillover regime. Under continuous spillover, repeated external seeding interacts with within-human transmission to produce a more diffuse and less visually direct mapping between parameters and outcomes. This makes the continuous-spillover regime harder to interpret through simple monotone sensitivity summaries alone. This suggests that other parameters play an important role in shaping outbreak outcomes.

Epidemiologically, this distinction suggests that outbreak control depends not only on reducing human-to-human transmission after introduction but also on limiting repeated zoonotic seeding from the animal reservoir. In that sense, the model supports a dual control logic consistent with a One Health perspective (Royce & Fu, 2020).

Panel A: Single spillover ($M = 0$)

Param.	Sampling range	Mean	Median	Min	Max
T_E	Unif$(2, 21)$	11.4972	11.7143	2.0563	20.8301
T_I	Unif$(5, 16)$	10.3935	10.6500	5.0597	15.9674
R_0	Unif$(0.50, 1.59)$	1.0625	1.0567	0.5094	1.5682
N	Unif$(25000, 1.14 \times 10^6)$	577060	576732	25860	1.14×10^6
κ	0 if $M = 0$	0.0000	0.0000	0.0000	0.0000

Panel B: Continuous spillover ($M = 1$)

Param.	Sampling range	Mean	Median	Min	Max
T_E	Unif$(2, 21)$	11.5031	11.4472	2.4697	20.9750
T_I	Unif$(5, 16)$	10.6065	10.3546	5.0353	15.9478
R_0	Unif$(0.50, 1.59)$	1.0275	1.0226	0.5035	1.5870
N	Unif$(25000, 1.14 \times 10^6)$	587918	602718	34957	1.12×10^6
κ	Unif$(0.003, 0.079)$ if $M = 1$	0.0415	0.0412	0.0044	0.0789

Table 3: Summary of sampled input parameters by spillover regime.

Panel A: Single spillover ($M = 0$)

Output	Mean	Median	SD	Min	Max	Q95
Final size	1649.03	27.31	7046.37	1.48	58087.90	5805.80
Peak infectious	166.43	3.54	625.17	1.14	5437.90	883.77
Duration (days)	82.04	78.02	42.92	10.37	193.92	154.86
Pr(major outbreak)	0.164	0.160	0.122	0.000	0.480	0.380

Panel B: Continuous spillover ($M = 1$)

Output	Mean	Median	SD	Min	Max	Q95
Final size	586363	602605	334904	34957	1.12×10^6	1.09×10^6
Peak infectious	119288	103417	84076	5299	413994	273641
Duration (days)	314.75	338.08	58.92	153.37	377.91	371.85
Pr(major outbreak)	1.000	1.000	0.000	1.000	1.000	1.000

Table 4: Summary of simulation output statistics by spillover regime.

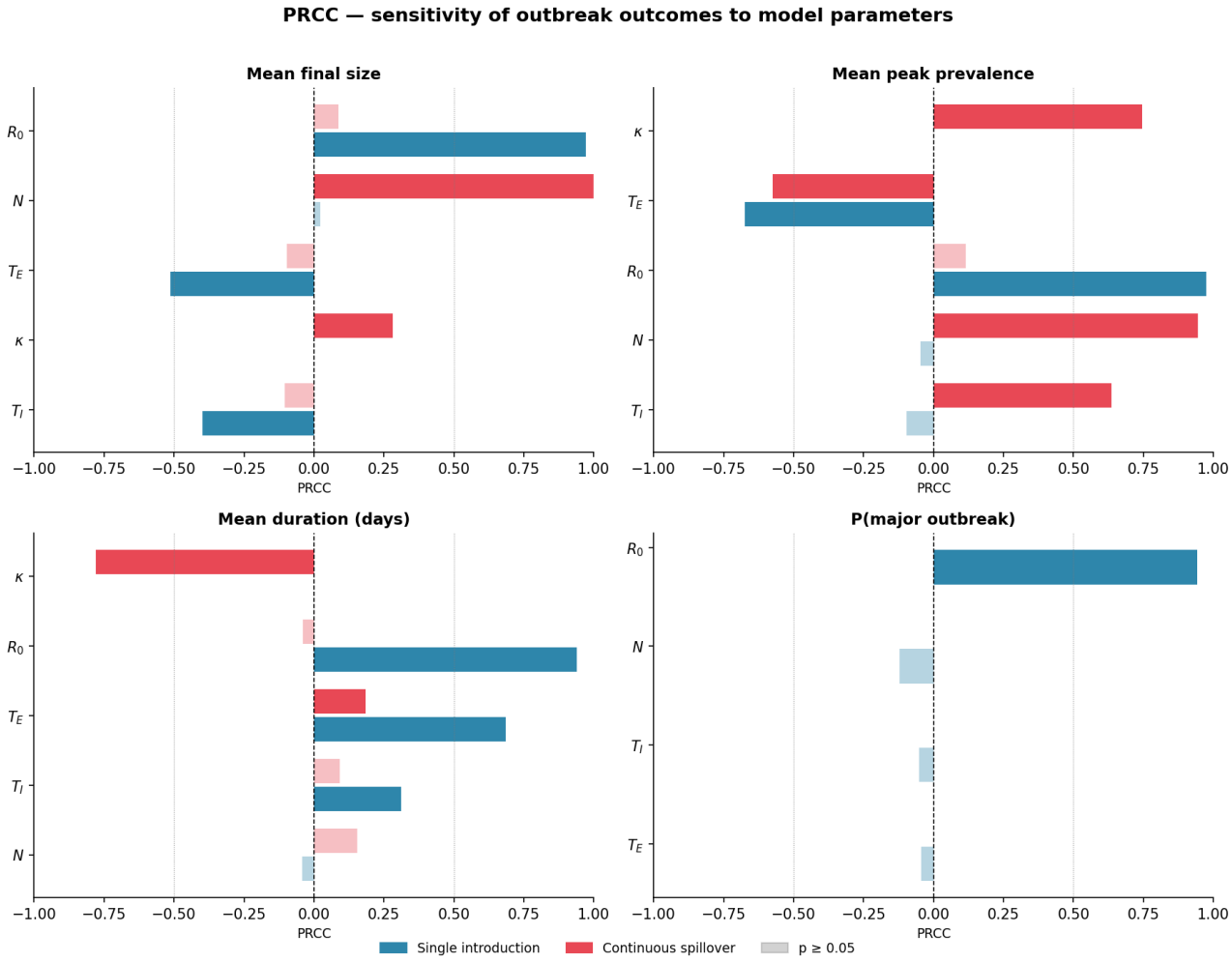

Figure 2: PRCC results for outbreak outcomes across single-introduction and continuous-spillover regimes.

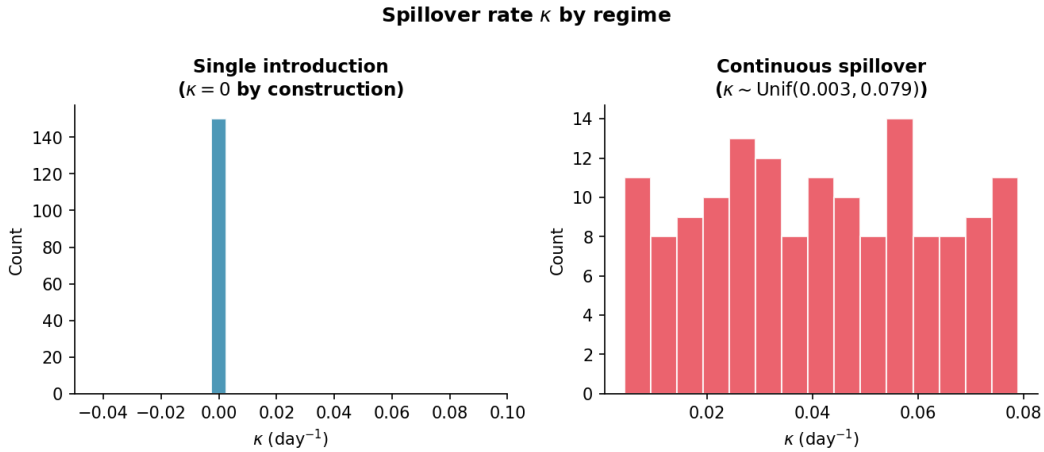

Figure 3: Distribution of the spillover rate κ by regime. Under single introduction, $\kappa = 0$ by construction, whereas under continuous spillover, κ is sampled over its prescribed range.

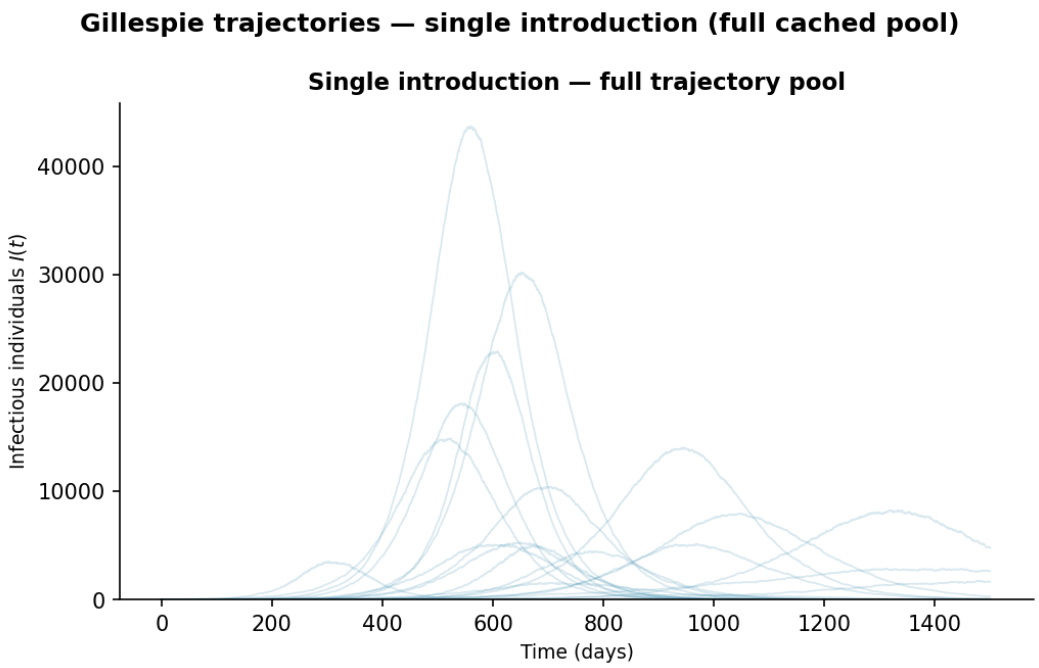

Figure 4: All cached Gillespie trajectories for the infectious compartment under the single-spillover regime.

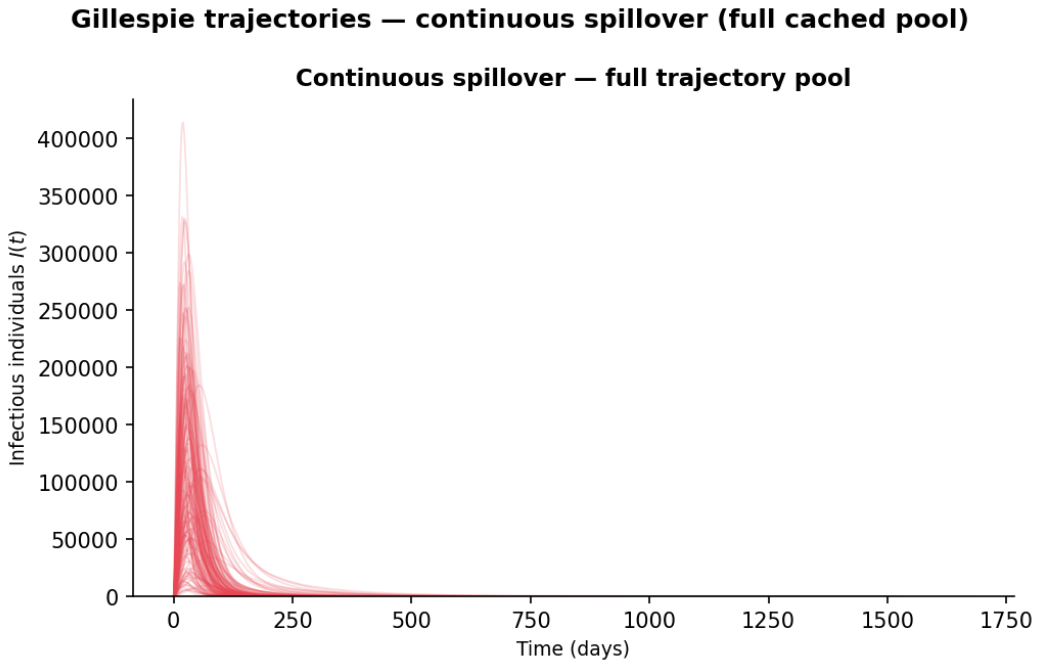

Figure 5: All cached Gillespie trajectories for the infectious compartment under the continuous-spillover regime.

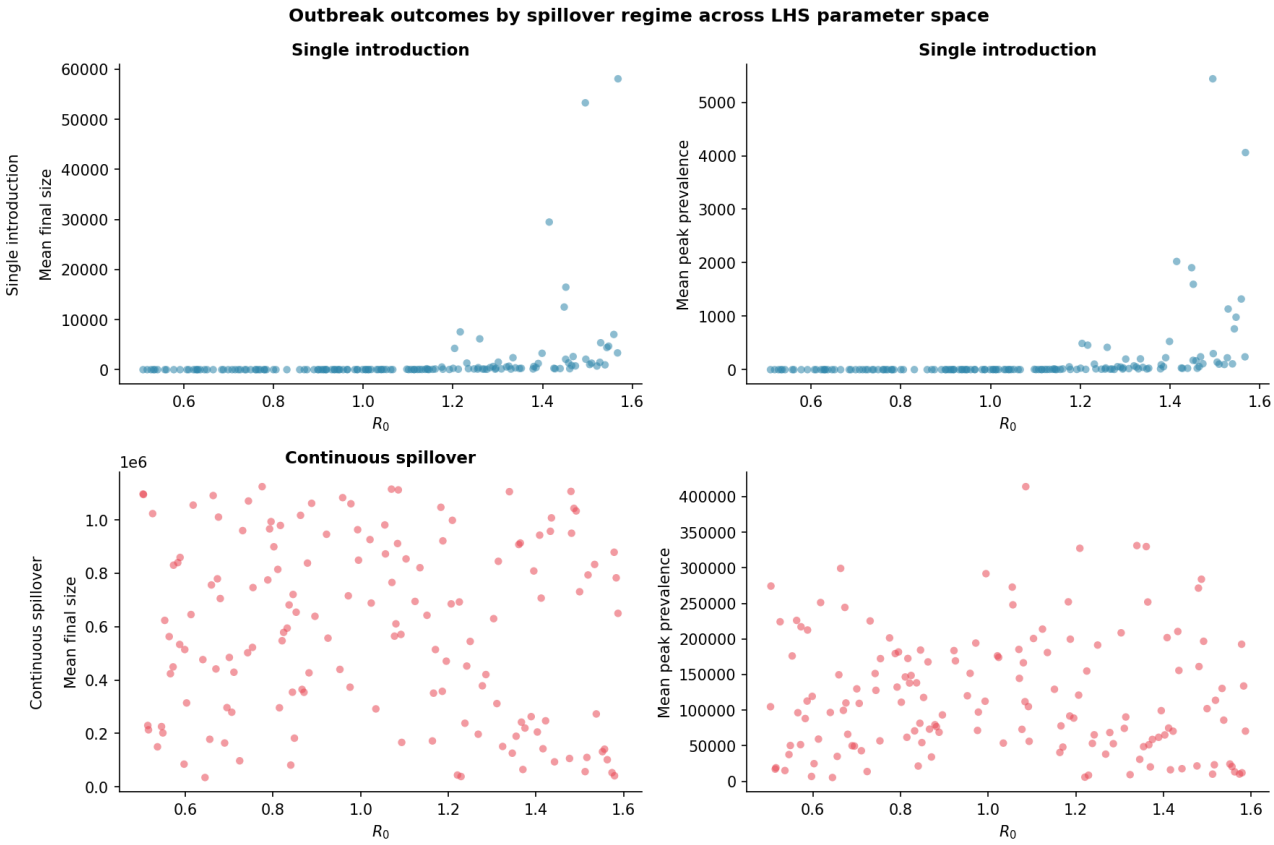

Figure 6: Scatterplots of outbreak outcomes across the sampled parameter space, stratified by spillover regime.

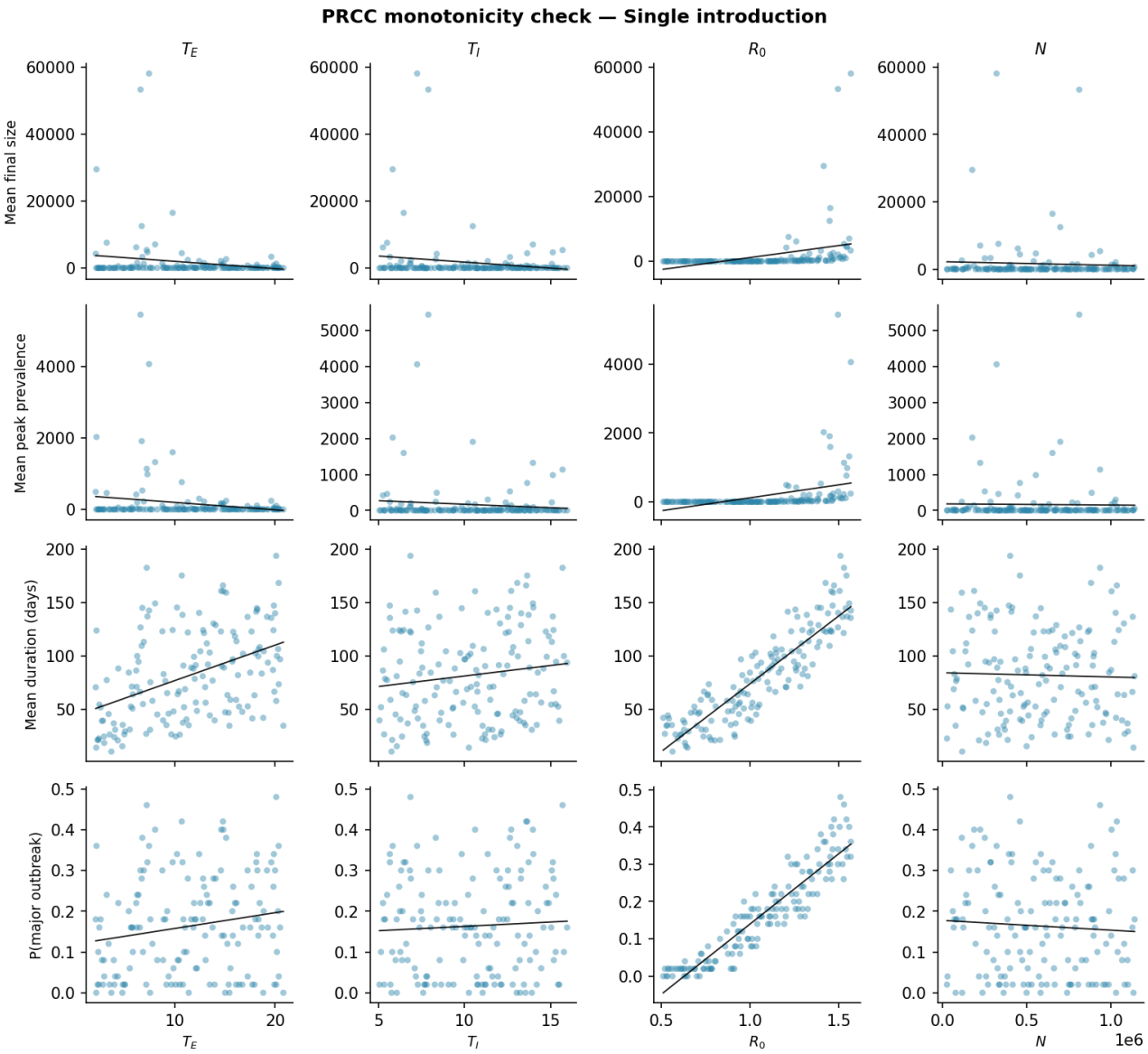

Figure 7: Monotonicity check plots for PRCC under the single-introduction regime. Each panel shows the relationship between one sampled input and one outbreak outcome.

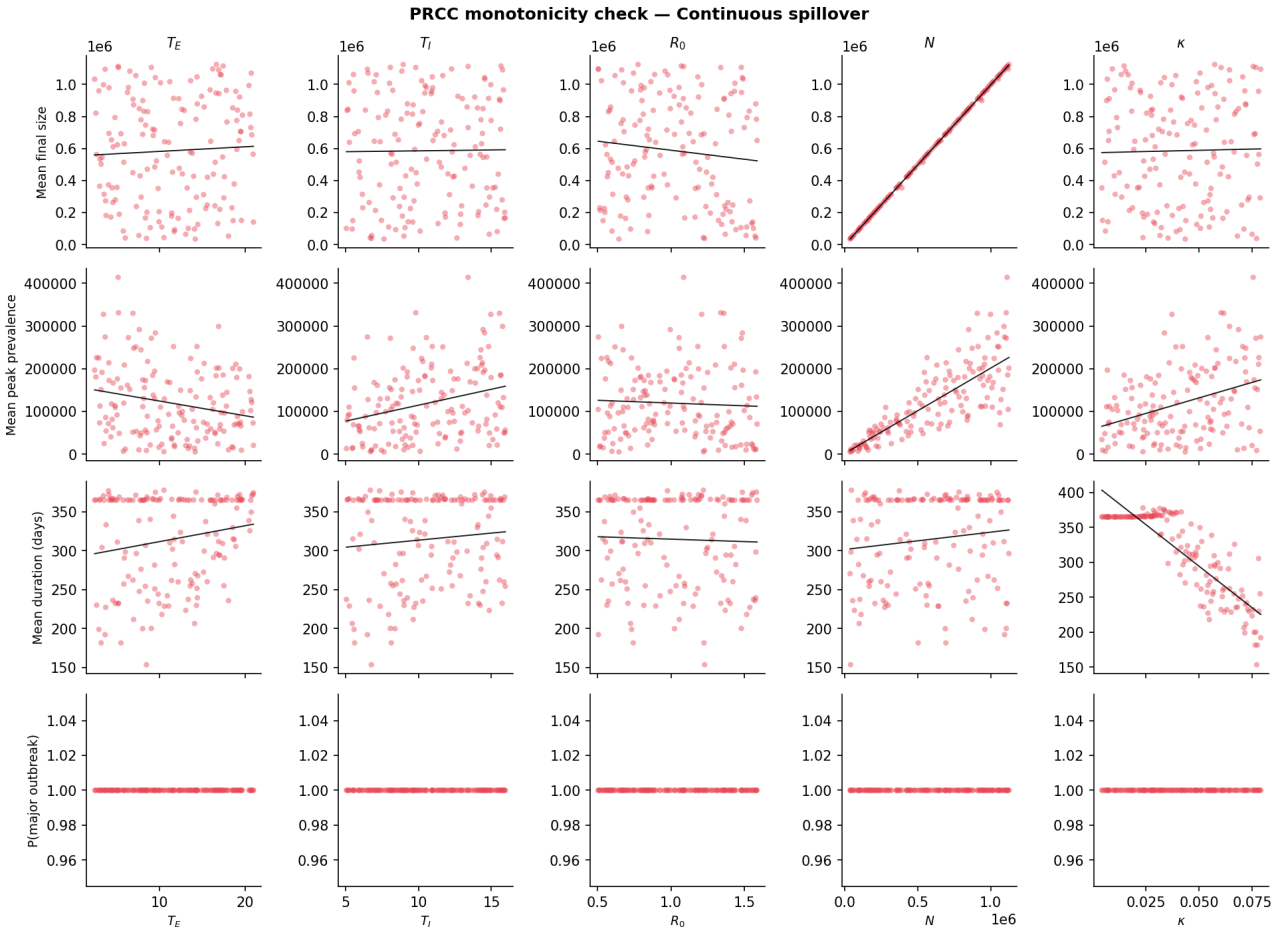

Figure 8: Monotonicity check plots for PRCC under the continuous-spillover regime. Each panel shows the relationship between one sampled input and one outbreak outcome.

Conclusion

This study used a stochastic SEIR-κ Gillespie framework to compare single-introduction and continuous-spillover regimes through LHS-PRCC, finding that repeated spillover produced substantially larger outbreaks, while single introductions produced longer outbreaks, less frequently, large epidemics.

Several limitations should be noted. The model assumes homogeneous mixing and therefore omits household, hospital, funeral, and spatial transmission structure. It is also transmission-focused rather than clinical, so the removed class combines recovery and death rather than representing disease severity explicitly, which is very important for public health given how large the CFR consistently is. In addition, the parameter ranges are exploratory rather than tightly calibrated to any single outbreak setting. Finally, sensitivity patterns under continuous spillover were less clearly monotone, so those results should be interpreted more cautiously.

Future work could investigate why stochastic comparisons of spillover regimes remain relatively uncommon in the literature, for example by extending similar analyses to more well-studied infectious diseases. This may help determine whether the gap reflects genuine biological simplification, limited data availability, or a broader modelling bias toward post-introduction human-to-human transmission. It would likewise be valuable to examine why rare but high-consequence diseases such as MVD continue to receive relatively limited modelling attention despite posing important public health risks, especially in contexts where repeated zoonotic introduction may shape outbreak dynamics. From a methodological perspective, further work could continue developing the LHS-based uncertainty framework through more principled distributional specification, and refined parameter selection methods. In addition, imputation-based strategies for incomplete data may provide a useful direction for improving parameter estimation and supporting calibration in data-sparse settings. Another extension would be to incorporate heterogeneous or spatially structured contact patterns, as the homogeneous-mixing framework likely oversimplifies the geographic and social realities of MVD transmission in sub-Saharan Africa, where outbreaks often unfold across unevenly connected villages, households, and healthcare settings.

Appendix

All simulations were implemented in Python. The core Gillespie simulation loop was greatly accelerated using Numba, a just-in-time (JIT) compiler for Python that translates numerical Python functions to native machine code at runtime via the LLVM compiler infrastructure. The main libraries used were NumPy for array operations, pandas for parameter set management and result aggregation, SciPy for LHS sampling and rank-based statistics, scikit-learn for the OLS regressions used in PRCC partialling, and Numba for JIT compilation and CPU parallelization. The code used in this study is available from the author only upon request, as the repository is still being organized and documented.

ChatGPT was used to format entries in the `.bib` file. No LLMs were used to generate results or make methodological decisions. This report was typeset using Quarto and the LaTeX engine is lualatex.

References

Ajelli, M., & Merler, S. (2012). Transmission potential and design of adequate control measures for marburg hemorrhagic fever. *PLOS ONE*, *7*(12), e50948. https://doi.org/10.1371/journal.pone.0050948

Allen, L. J. S. (2017). A primer on stochastic epidemic models: Formulation, numerical simulation, and analysis. *Infectious Disease Modelling*, *2*(2), 128–142. https://doi.org/10.1016/j.idm.2017.03.001

Allen, L. J. S., Brown, V. L., Jonsson, C. B., Klein, S. L., Laverty, S. M., Magwedere, K., Owen, J. C., & Driessche, P. van den. (2012). Mathematical modeling of viral zoonoses in wildlife. *Natural Resource Modeling*, *25*(1), 5–51. https://doi.org/10.1111/j.1939-7445.2011.00104.x

Bausch, D. G., Nichol, S. T., Muyembe-Tamfum, J. J., Borchert, M., Rollin, P. E., Sleurs, H., Campbell, P., Tshioko, F. K., Roth, C., Colebunders, R., Pirard, P., Mardel, S., Ollevier, F., Kasin, S., Kibadi, K., Kawata, A. K., Torfason, E. G., Formenty, P., Shieh, W.-J., … Ksiazek, T. G. (2006). Marburg hemorrhagic fever associated with multiple genetic lineages of virus. *New England Journal of Medicine*, *355*(9), 909–919. https://doi.org/10.1056/NEJMoa051465

Borchert, M., Mulangu, S., Swanepoel, R., Libande, M. L., Tshomba, A., Kulidri, A., Muyembe-Tamfum, J.-J., & Van der Stuyft, P. (2006). Serosurvey on household contacts of marburg hemorrhagic fever patients. *Emerging Infectious Diseases*, *12*(3), 433–439. https://doi.org/10.3201/eid1203.050622

Callendret, B., Vellinga, J., Wunderlich, K., Rodriguez, A., Steigerwald, R., Dirmeier, U., Cheminay, C., Volkmann, A., Brasel, T., Carrion, R., Giavedoni, L. D., Patterson, J. L., Mire, C. E., Geisbert, T. W., Hooper, J. W., Weijtens, M., Hartkoorn-Pasma, J., Custers, J., Pau, M. G., … Zahn, R. (2018). A prophylactic multivalent vaccine against different filovirus species is immunogenic and provides protection from lethal infections with ebolavirus and marburgvirus species in non-human primates. *PLOS ONE*, *13*(2), e0192312. https://doi.org/10.1371/journal.pone.0192312

Carmona, S. (2025, September). *Ebola virus and marburg virus infections*. Merck Manual Consumer Version. https://www.merckmanuals.com/home/infections/arboviruses-arenaviruses-filoviruses/ebola-virus-and-marburg-virus-infections

Centers for Disease Control and Prevention. (2025a). *History of marburg outbreaks*. https://www.cdc.gov/marburg/outbreaks.

Centers for Disease Control and Prevention. (2025b, January 31). *History of marburg outbreaks*. National Center for Emerging; Zoonotic Infectious Diseases. https://www.cdc.gov/marburg/outbreaks/index.html

Cuomo-Dannenburg, G., McCain, K., McCabe, R., Unwin, H. J. T., Doohan, P., Nash, R. K., Hicks, J. T., Charniga, K., Geismar, C., Lambert, B., Nikitin, D., Skarp, J., Wardle, J., Kont, M., Bhatia, S., Imai, N., Elsland, S. van, Cori, A., Morgenstern, C., & Group, P. E. R. (2024). Marburg virus disease outbreaks, mathematical models, and disease parameters: A systematic review. *The Lancet Infectious Diseases*, *24*(5), e307–e317. https://doi.org/10.1016/S1473-3099(23)00515-7

Data Commons. (2016). *Uíge province — demographics*. https://datacommons.org/place/wikidataId/Q216972

European Centre for Disease Prevention and Control. (2024, October 10). *Factsheet for health professionals about marburg virus disease*. European Centre for Disease Prevention; Control. https://www.ecdc.europa.eu/en/infectious-disease-topics/marburg-virus-disease/factsheet-health-professionals-about-marburg-virus

IAVI. (2026). *Marburg virus vaccine*. https://www.iavi.org/our-work/emerging-infectious-diseases/marburg-virus-vaccine/

Keeling, M. J., & Rohani, P. (2008). *Modeling infectious diseases in humans and animals*. Princeton University Press.

O'Neill, R. (2024). *Nonprofits lead the way on marburg vaccines*. https://www.politico.eu/article/marburg-vaccine-health-virus-rwanda-nonprofit/.

Odatalla, S. (2020). *Stochastic modeling of zoonotic disease*. Montclair State University; Theses, Dissertations and Culminating Projects, 474. https://digitalcommons.montclair.edu/etd/474

Pavlin, B. I. (2014). Calculation of incubation period and serial interval from multiple outbreaks of marburg virus disease. *BMC Research Notes*, *7*, 906. https://doi.org/10.1186/1756-0500-7-906

Qian, G. Y., Edmunds, W. J., Bausch, D. G., et al. (2023). A mathematical model of marburg virus disease outbreaks and the potential role of vaccination in control. *BMC Medicine*, *21*, 439. https://doi.org/10.1186/s12916-023-03108-x

Royce, K., & Fu, F. (2020). Mathematically modeling spillovers of an emerging infectious zoonosis with an intermediate host. *PLOS ONE*, *15*(8), e0237780. https://doi.org/10.1371/journal.pone.0237780

Soni, S., & Rathish, B. (2026). Marburg virus disease. In *StatPearls [internet]*. StatPearls Publishing. https://www.ncbi.nlm.nih.gov/books/NBK578176/

Teshome, G. S., Ketema, T. G., Uwimana, P., Kayiranga, D., Rugema, J., Murekatete, A., Manirafasha, J. P., & Mukandayisaba, D. (2025). Exploring the epidemiology, transmission dynamics and public health interventions of marburg viral disease: A scoping review of global evidence. *Rwanda Journal of Medicine and Health Sciences*, *8*(2), 420–433. https://doi.org/10.4314/rjmhs.v8i2.20

World Health Organization. (2025, January 20). *Marburg virus disease*. World Health Organization. https://www.who.int/news-room/fact-sheets/detail/marburg-virus-disease

World Health Organization. (2026a). *Marburg virus disease*. https://www.who.int/news-room/fact-sheets/detail/marburg-virus-disease

World Health Organization. (2026b). *Prioritizing diseases for research and development in emergency contexts*. https://www.who.int/activities/prioritizing-diseases-for-research-and-development-in-emergency-contexts